

ExDet: Open-Domain Open-Vocabulary Detection with Cross-modal Extrapolation and Rectification

Yupeng Zhang
College of Intelligence and
Computing, Tianjin University
Tianjin, China
zhangyupeng@tju.edu.cn

Yuzhong Feng
College of Intelligence and
Computing, Tianjin University
Tianjin, China
yzfeng@tju.edu.cn

Ruize Han
Faculty of Computer Science and
Artificial Intelligence, Shenzhen
University of Advanced Technology
Shenzhen, China
hanruize@suat-sz.edu.cn

Zhiwei Chen
School of Artificial Intelligence,
Nanchang University
Jiangxi, China
zhiweichen@ncu.edu.cn

Wei Feng
College of Intelligence and
Computing, Tianjin University
Tianjin, China
wfeng@ieee.org

Liang Wan
College of Intelligence and
Computing, Tianjin University
Tianjin, China
lwan@tju.edu.cn

Abstract

Open-domain open-vocabulary detection (ODOVD) requires detectors to generalize to both novel categories and unseen domains, making it more challenging than open-vocabulary detection. Existing methods typically train open-vocabulary detectors together with domain generalization modules from scratch, leading to high training cost. We propose ExDet, a lightweight category-domain collaborative generalization framework for ODOVD that enhances the cross-category and cross-domain generalization of existing detectors. ExDet consists of Text-Guided Extrapolation (TGE), a lightweight Detector-Compatible Rectification (DCR) module, and ExRPN. Specifically, TGE exploits the DeltaSpace property of vision-language models (VLMs) to infer category- and domain-aware proxy visual prototypes from text. DCR is learned from the TGE-generated prototypes in a detector training-free and real-data-free manner, and is inserted after the classification head at inference to rectify representations toward a detector-compatible source-domain visual distribution, thereby enhancing classification for targets from novel categories and unseen domains. ExRPN recalibrates proposal scores by combining semantic similarity with RPN confidence, improving recall for novel and domain-shifted objects while providing better support for subsequent classification and DCR. ExDet achieves SOTA performance on OD-LVIS, OV-LVIS, Objects365, and MSOSB.

CCS Concepts

• **Computing methodologies** → **Artificial intelligence**; **Computer vision**; **Object detection**;

Permission to make digital or hard copies of all or part of this work for personal or classroom use is granted without fee provided that copies are not made or distributed for profit or commercial advantage and that copies bear this notice and the full citation on the first page. Copyrights for components of this work owned by others than the author(s) must be honored. Abstracting with credit is permitted. To copy otherwise, or republish, to post on servers or to redistribute to lists, requires prior specific permission and/or a fee. Request permissions from permissions@acm.org.

MM '26, Janeiro, Brazil

© 2026 Copyright held by the owner/author(s). Publication rights licensed to ACM.
ACM ISBN 978-1-4503-XXXX-X/2018/06
<https://doi.org/XXXXXXX.XXXXXXX>

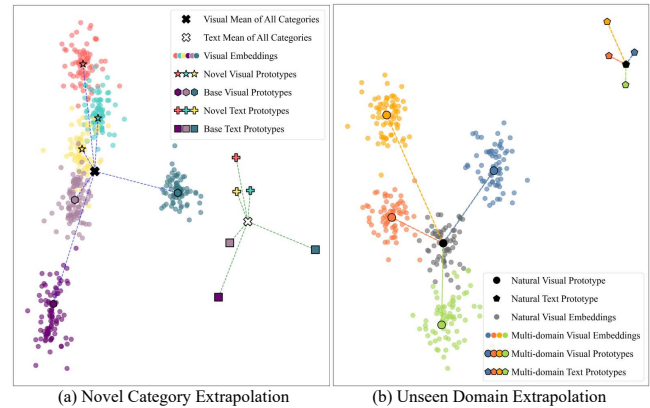


Figure 1: PCA visualization of visual extrapolation for novel categories and unseen domains, where text and image features are slightly shifted in the shared representation space for clarity. (a) Novel Category Extrapolation: The relative distribution of base and novel categories in the text space is consistent with that of their corresponding visual prototypes in the visual space. (b) Unseen Domain Extrapolation: For the same category, the offset from multi-domain text prototypes to the natural text prototype corresponds structurally to the offset from the corresponding visual prototypes to the natural-domain visual prototype.

Keywords

Open Domain, Open Vocabulary, Object Detection, VLMs

ACM Reference Format:

Yupeng Zhang, Yuzhong Feng, Ruize Han, Zhiwei Chen, Wei Feng, and Liang Wan. 2026. ExDet: Open-Domain Open-Vocabulary Detection with Cross-modal Extrapolation and Rectification. In *Proceedings of the 34th ACM International Conference on Multimedia (MM '26)*. ACM, New York, NY, USA, 11 pages. <https://doi.org/XXXXXXX.XXXXXXX>

1 Introduction

In recent years, object detection has achieved remarkable progress under supervised learning. However, existing methods largely rely

on large-scale manual annotations and assume a predefined closed-set label space, making them inadequate for real-world scenarios with ever-expanding object categories. To address this limitation, Open-Vocabulary Detection (OVD) [49] leverages the open semantic representations of vision-language models (VLMs) [14, 28] to generalize from limited annotated categories to unseen ones. However, distribution shifts in real applications often go beyond category shift alone and are frequently accompanied by visual domain shift [22], resulting in the more challenging setting of joint category-domain shift. For example, when a detector trained on indoor scenes is deployed in outdoor environments, object categories, illumination, weather, and overall imaging style may all change simultaneously. To tackle this challenge, Open-Domain Open-Vocabulary Detection (ODOVD) [52] has been introduced to achieve unified object detection generalization across both categories and domains.

Although DVtor [52], the pioneering work on ODOVD, improves cross-domain robustness by introducing a domain grafting mechanism, it requires joint training with the detector, leading to increased training cost and system complexity. In fact, DVtor mainly focuses on enhancing classification capability, while paying limited attention to proposal generation in two-stage detectors. In practice, the Region Proposal Network (RPN) is trained only on base-category annotations from the source domain, and thus often struggles to produce high-quality, high-confidence proposals for novel or domain-shifted objects. As a result, many latent objects are filtered out before reaching the RoI head. Therefore, the challenge of ODOVD lies not only in improving classification for novel categories and unseen domains, but also in enhancing proposal recall for novel and domain-shifted objects.

We observe that the text and visual spaces of VLMs are not isolated, but exhibit structural correspondence. In particular, DeltaSpace [25, 26] suggests that directional changes in the text semantic space can translate into semantic shifts in the visual space. Although prior studies [2, 23, 37, 41] have validated the effectiveness of DeltaSpace in image editing and related tasks, its applicability to object detection remains underexplored. Furthermore, as shown in Fig. 1, our preliminary visualization reveals that, *at the object-concept level, category- and domain-induced text semantic shifts exhibit a broadly consistent structural relationship with feature shifts in the visual space*. Motivated by this observation, we ask a key question: *can we infer proxy visual prototypes for novel categories and unseen domains solely from category and domain descriptions, and design a lightweight compatibility module to enhance cross-category and cross-domain generalization in a detector training-free and real-data-free manner?*

Based on the above observations, we propose ExDet, a lightweight enhancement framework for ODOVD. By combining text-guided visual extrapolation, Detector-Compatible Rectification, and inference-time proposal rectification, ExDet addresses two key bottlenecks of two-stage detectors under joint category-domain shifts: 1) insufficient discrimination of the classification head for novel categories and unseen domains, and 2) limited proposal recall for novel and domain-shifted objects. Without retraining the detector, ExDet effectively improves both cross-category and cross-domain generalization. Specifically, to address the former, we introduce **Text-Guided Extrapolation (TGE)** and **Detector-Compatible Rectification (DCR)**. TGE exploits the distributional relationships

of text embeddings in the VLM feature space to extrapolate cross-category, cross-domain proxy visual prototypes. DCR is independently trained under the supervision of enhanced prototypes and, in a **detector training-free** and **real-data-free** manner, rectifies post-classification-head representations toward a detector-compatible source-domain visual distribution, thereby improving discrimination for objects from novel categories and unseen domains. To address the latter, we further introduce ExRPN, a complementary inference-time strategy that semantically rectifies proposal confidence scores to improve recall for novel and domain-shifted objects while providing better candidate support for subsequent classification and rectification.

In summary, the main contributions of this paper are as follows:

- We propose ExDet, a lightweight framework for ODOVD that enhances the cross-category and cross-domain generalization of existing two-stage detectors under joint category-domain shifts in a detector training-free and real-data-free manner.
- We design a framework consisting of Text-Guided Extrapolation (TGE), a lightweight Detector-Compatible Rectification (DCR) module trained independently of the detector, and ExRPN. TGE constructs category- and domain-aware proxy visual prototypes from text descriptions; DCR rectifies classification representations toward a detector-compatible source-domain visual distribution for better discrimination of novel categories and unseen domains; and ExRPN recalibrates proposal confidence at inference to improve recall of novel and domain-shifted objects while supporting subsequent classification and rectification.
- Extensive experiments on OD-LVIS [52], OV-LVIS [10], Objects365 [31], and MSOSB [53] demonstrate that our method achieves SOTA performance and strong generalization under both category and domain shifts. ExDet also trains in only about 30 minutes on a single RTX 3090 GPU.

2 Related Work

Open-Vocabulary Detection (OVD). With the rapid development of VLMs such as CLIP [28] and ALIGN [14], OVD [49] has become an important research direction, aiming to recognize both base and novel categories within a unified cross-modal semantic space. Existing methods mainly rely on knowledge distillation, large-scale region-text supervision, transfer learning, or pseudo-labeling. For example, ViLD [9], DetPro [6], OADP [38], and DK-DETR [21] distill CLIP knowledge into detectors, while RO-ViT [16], CORA [43], YOLO-World [4], and YOLOE [34] improve open-world perception with large-scale region-text data, albeit at high cost. Pseudo-labeling methods, such as Detic [57], OCO [1], ProxyDet [13], LBP [20], SAS-Det [54], and OV-DQUO [35], mine potential objects from image-level tags, class-agnostic detectors, or proxy categories, but their reliance on text matching often introduces noise and limits generalization to novel categories. Meanwhile, F-VLM [18], CLIPSelf [42], DST-Det [46], NoOVD [51], and DeCLIP [36] build two-stage detectors on frozen CLIP models, training only the detection heads for open-vocabulary recognition. As the first ODOVD method, DVtor [52] also builds on frozen VLMs, better preserving the category- and domain-generalization ability inherited from VLM pre-training.

Building on this paradigm, we introduce a Detector-Compatible Rectification (DCR) module after the classification head to improve inference-time generalization to novel categories and unseen domains, together with ExRPN to recalibrate proposal confidence scores and enhance recall for novel and domain-shifted objects.

Domain Generalization (DG) based object detection aims to train detectors on source domains that generalize to unseen target domains. Early works explored feature disentanglement for cross-domain generalization [22], and Gated Disentangling Network [50] further improved generalization by activating domain-invariant channels. However, these methods rely on data and annotations from multiple source domains. In contrast, single-domain generalized object detection (SDGOD) [39] considers the more challenging setting where only one source domain is available. Existing SDGOD methods can be broadly categorized into four groups. Data augmentation methods, such as CLIP the Gap [33], DivAlign [5], and SRCD [29], improve robustness by expanding the training distribution with image- or feature-level perturbations, but often still rely on two-stage detectors or auxiliary modules. Feature disentanglement methods, including SDGOD [39], DG-DETR [12], and UFR [24], separate domain-invariant and domain-specific factors through dedicated architectures or objectives, yet usually introduce additional computation or inference branches. Architecture search methods, such as G-NAS [40], seek detector structures more favorable for generalization, while test-time adaptation methods, e.g., SA-DETR [11], adapt models to unseen domains through dynamic inference-time adjustment, at the cost of extra overhead. Our setting is closely related to SDGOD, with training on a single source domain and evaluation across multiple open domains. Unlike conventional DG-based detectors, we address the more challenging ODOVD setting, which demands simultaneous generalization to novel categories and unseen domains.

Semantic DeltaSpace of VLMs. VLMs, especially CLIP [28], have shown strong cross-modal representation and alignment ability by learning a unified semantic space from large-scale image-text pairs. Recent studies [2, 23, 25, 26, 37, 41] show that, in the semantic DeltaSpace of VLMs, shifts in text embeddings can partially induce corresponding shifts in visual embeddings. Inspired by this, we propose TGE to extrapolate proxy visual features for novel categories and unseen domains from textual semantic relations, together with a lightweight DCR module that rectifies them toward a detector-compatible source-domain visual distribution, thereby improving generalization to targets from novel categories and unseen domains in a detector training-free and real-data-free manner.

3 Proposed Method

3.1 Preliminaries and Framework

Problem formulation. During the training stage, we use the data from the *single source domain* (i.e., the natural scenes). Specifically, the training image dataset is notated as $\mathcal{D}^{\text{train}} = \{\mathbf{I}_i^{\text{train}}, L_i\}_{i=1}^N$, where N is the number of training images, \mathbf{I}_i denotes an image from the source domain with the detection annotation L_i for it. The label L_i is composed of $\{\mathbf{b}_i, \mathbf{c}_i\}$, in which \mathbf{b}_i indicates all the annotated object bounding boxes in \mathbf{I}_i , and the corresponding object categories are stored in \mathbf{c}_i . Note that, all the (annotated) object categories contained in L_i of the training set $\mathcal{D}^{\text{train}}$ are from the *base*

category set, i.e., $\mathcal{C}^{\text{base}}$. During the testing stage, the ODOVD task requires the model to operate under both *open-domain* and *open-vocabulary* conditions. Specifically, the test images are sampled from hybrid open domains (i.e., exhibiting diverse image styles), denoted as $\mathcal{D}^{\text{test}} = \{\mathbf{I}_j^{\text{test}}\}_{j=1}^M$, where M is the dataset scale. For each test image $\mathbf{I}_j^{\text{test}}$, the model is expected to output a set of predicted object bounding boxes and their corresponding categories, i.e., $\{\mathbf{b}_j, \mathbf{c}_j\}$. Following the OVD setting, the predicted categories include both the *base categories* $\mathcal{C}^{\text{base}}$ (seen during training) and the *novel categories* $\mathcal{C}^{\text{novel}}$ (unseen during training), which together form the *open-vocabulary category set*, defined as: $\mathcal{C}^{\text{open}} = \mathcal{C}^{\text{base}} + \mathcal{C}^{\text{novel}}$.

Overview. In Fig. 2, we propose ExDet, a lightweight category-domain co-generalization framework built upon a frozen two-stage open-vocabulary detector. It consists of three key components: Text-Guided Extrapolation (TGE), Detector-Compatible Rectification (DCR), and ExRPN. Specifically, TGE exploits the DeltaSpace property of VLMs to extrapolate category-aware and domain-aware proxy visual prototypes, while DCR is independently trained under the supervision of these enhanced prototypes and plugged into the detector at inference to rectify post-classification-head region representations toward a detector-compatible source-domain visual distribution, thereby improving classification of targets from novel categories and unseen domains. As a complementary inference-time strategy, ExRPN recalibrates proposal scores based on the similarity between proposal features and multi-domain semantic descriptions, improving recall for novel and domain-shifted objects while providing better candidate support for subsequent classification and DCR. Overall, ExDet improves the cross-category and cross-domain generalization ability of existing detectors in a **detector training-free** and **real-data-free** manner.

3.2 Text-Guided Extrapolation

Since the training data cover only base categories in a single source domain, the detector lacks direct exposure to the visual variations of novel categories and unseen domains. To address this limitation without introducing additional real data, we propose **Text-Guided Extrapolation (TGE)** in the semantic space of VLMs, as shown on the left of Fig. 2. By exploiting the DeltaSpace [25, 26] property of VLMs, TGE synthesizes proxy visual prototypes for both novel categories and unseen domains.

Novel category prototype extrapolation. We first encode all test categories using a fixed text template with a pre-trained VLM (e.g., CLIP). For base categories, we extract the corresponding visual embeddings from the frozen detector’s classification head, normalize them, and average them to obtain a base-category visual prototype. We then transfer the offset between the novel-category text prototype and the base-category text prototype into the visual space to obtain the visual prototype of each novel category.

Specifically, let t_n denote the text prototype of novel category n , and \bar{t}_b and \bar{v}_b the base-category text and visual prototypes. The extrapolated visual prototype for category n is defined as

$$\hat{v}_n = \bar{v}_b + (t_n - \bar{t}_b). \quad (1)$$

This linear extrapolation requires no additional training and provides zero-shot proxy visual prototypes for novel categories.

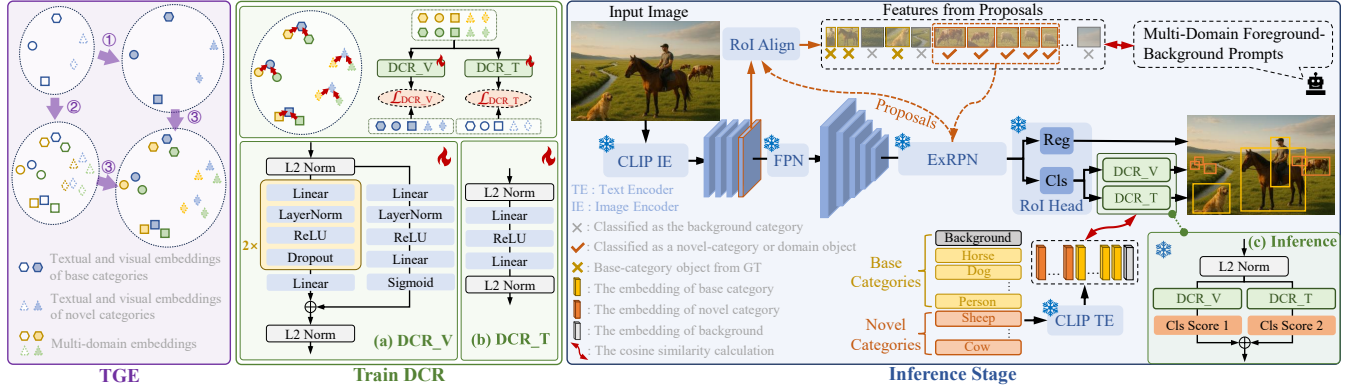


Figure 2: Overview of ExDet. Built upon a frozen F-ViT detector, ExDet is a lightweight category-domain generalization framework consisting of Text-Guided Extrapolation (TGE), Detector-Compatible Rectification (DCR), and ExRPN. TGE (①–③) generates enhanced embeddings covering novel categories and diverse domains to train DCR independently, where DCR comprises a visual branch (DCR_V) for source-domain visual alignment and a semantic branch (DCR_T) for preserving compatibility with the text space. During inference, DCR is inserted after the classification head to improve category-domain generalization. To further enhance recall for novel and domain-shifted objects, ExRPN recalibrates proposal confidence scores using coarse-grained semantic prompts adopted from NoVD.

Domain-aware text prototype construction. To simulate visual domain variations commonly encountered in real-world scenarios, we construct a diverse set of domain labels $\{D_j\}_{j=1}^N$ (e.g., ‘rainy’, ‘blurry’, ‘oil painting’). These labels are combined with category names under a unified template, ‘a [domain] image of a/an [category]’, to form multi-domain textual descriptions. We then encode these descriptions with a pre-trained VLM (e.g., CLIP) to obtain the corresponding domain-aware text prototypes, denoted as $t_{c,j}^D$, where c indexes the category (including both base and novel categories) and j indexes the domain type.

Cross-domain visual prototype generation. Moreover, we synthesize domain-aware visual prototypes by combining each category’s visual prototype with the relative shift between its domain-specific and general text prototypes. Similar to category extrapolation, we assume that the offset between a category’s domain-specific text prototype and its general text prototype, i.e., $\Delta_{c,j}^D = t_{c,j}^D - t_c$, can be approximately transferred to the visual space. By adding this offset to the visual prototype of category c , we obtain its domain-aware visual prototype under domain j :

$$\hat{v}_{c,j}^D = \hat{v}_c + \Delta_{c,j}^D, \quad (2)$$

where $\hat{v}_{c,j}^D$ denotes the domain-aware visual prototype of category c under domain j , t_c denotes the general text prototype of category c , and \hat{v}_c denotes the category visual prototype obtained from Eq. (1), including those synthesized for novel categories. To further enrich diversity, we additionally construct mixed-domain visual prototypes through randomized weighted combinations of different domain-aware visual prototypes.

3.3 Detector-Compatible Rectification

TGE constructs category- and domain-aware augmented visual prototypes, thereby compensating for the missing visual variations of novel categories and unseen domains **without introducing additional real data**. However, these text-guided synthesized features are not naturally compatible with the original detector’s classification space. To make them effectively usable, we employ them as

supervision to train a lightweight **Detector-Compatible Rectification (DCR)** network; during inference, DCR operates on the post-classification-head representations of candidate regions and rectifies them to the detector-compatible source-domain visual distribution while preserving category discriminability. As shown in the middle of Fig. 2, DCR consists of two complementary branches: a visual branch (DCR_V) for source-domain prototype rectification and a text branch (DCR_T) for semantic consistency with the frozen text classifier.

Visual branch: DCR_V. As illustrated in Fig. 2 (a), DCR_V adopts a gated residual architecture to rectify the TGE-generated domain-aware visual prototypes to the corresponding source-domain category prototypes. Given an input prototype $\hat{v}_{c,j}^D$, DCR_V outputs a refined representation $\tilde{v}_{c,j}^{D,v}$.

The main branch of DCR_V consists of two stacked feed-forward layers that model nonlinear distribution shifts, while an auxiliary gating branch produces a modulation vector to adaptively control the transformation. The outputs of the two branches are combined through residual addition, allowing DCR_V to preserve category identity while correcting domain-induced deviations.

The DCR_V is trained with three complementary objectives:

Cosine-based cross-entropy loss. This loss encourages the refined prototype to be discriminatively aligned with the correct source-domain category prototype:

$$\mathcal{L}_{CE}^{(v)} = -\log \frac{\exp(\cos(\tilde{v}_{c,j}^{D,v}, \hat{v}_c)/\tau)}{\sum_{c'} \exp(\cos(\tilde{v}_{c,j}^{D,v}, \hat{v}_{c'})/\tau)}, \quad (3)$$

where $\hat{v}_{c'}$ denotes the source-domain visual prototypes of all categories, and τ is a temperature hyperparameter.

L2 reconstruction loss. To minimize the distance between the refined prototype and its source-domain counterpart, we use

$$\mathcal{L}_{L2}^{(v)} = \|\tilde{v}_{c,j}^{D,v} - \hat{v}_c\|_2^2. \quad (4)$$

Contrastive loss. To improve inter-category separability and reduce feature confusion, we adopt a supervised contrastive objective:

$$\mathcal{L}_{\text{con}}^{(v)} = \sum_{i \in \mathcal{I}} \frac{-1}{|\mathcal{P}(i)|} \sum_{p \in \mathcal{P}(i)} \log \frac{\exp(z_i \cdot z_p / \tau)}{\sum_{a \in \mathcal{A}(i)} \exp(z_i \cdot z_a / \tau)}, \quad (5)$$

where \mathcal{I} denotes the index set of all samples in a batch, $\mathcal{P}(i)$ is the set of positive samples sharing the same label as anchor i , $\mathcal{A}(i)$ is the set of all comparison samples for anchor i , and z_i , z_p , and z_a denote the anchor, positive, and comparison embeddings, respectively.

The overall objective of DCR_V is

$$\mathcal{L}_{\text{DCR_V}} = \mathcal{L}_{\text{CE}}^{(v)} + \mathcal{L}_{\text{L2}}^{(v)} + \mathcal{L}_{\text{con}}^{(v)}. \quad (6)$$

Together, the cosine-based cross-entropy, L2 reconstruction, and contrastive losses improve category discriminability, enforce source-domain prototype alignment, and enhance feature-space separability, respectively, thereby facilitating effective rectification to the detector-compatible source-domain visual distribution.

Text branch: DCR_T. As shown in Fig. 2 (b), DCR_T aligns the augmented visual prototypes with the textual semantic space, keeping the refined features compatible with the frozen text classifier. Given the same input prototype $\hat{v}_{c,j}^D$, it produces a refined representation $\tilde{v}_{c,j}^{D,t}$ through a lightweight feed-forward mapping.

DCR_T is optimized with a cosine-based cross-entropy loss:

$$\mathcal{L}_{\text{DCR_T}} = \mathcal{L}_{\text{CE}}^{(t)} = -\log \frac{\exp(\cos(\tilde{v}_{c,j}^{D,t}, t_c) / \tau)}{\sum_{c'} \exp(\cos(\tilde{v}_{c,j}^{D,t}, t_{c'}) / \tau)}, \quad (7)$$

where $t_{c'}$ denotes the text prototypes of all categories, and τ is the temperature hyperparameter.

Unlike DCR_V, which focuses on rectifying enhanced prototypes toward a detector-compatible source-domain visual distribution, DCR_T aims to preserve semantic consistency with the frozen text classifier. Therefore, we optimize DCR_T only with a cosine-based cross-entropy loss, which encourages the refined visual prototypes to remain close to the correct text prototypes while being separable from those of other categories.

Application of DCR. As shown in Fig. 2 (c), during inference we insert the trained DCR branches after the original classification head. For each proposal feature, DCR_V and DCR_T produce branch-specific refined representations, from which visual- and text-prototype-based classification scores are computed, respectively. The final score is obtained by weighted fusion of the two branches. In this way, DCR improves compatibility with both the source-domain visual distribution and the frozen text classifier, enabling efficient generalization to novel categories and unseen domains in a **detector training-free** and **real-data-free** manner.

3.4 ExRPN for Category and Domain Shift

To alleviate the low recall of novel and domain-shifted objects at the proposal stage—which directly limits subsequent classification and rectification—we adopt the R-RPN design of NoOVD [51] and extend it to the multi-domain setting, yielding a lightweight inference-time proposal confidence rectification strategy termed ExRPN. It recalibrates proposal confidence before post-processing, increasing the probability that proposals containing novel and domain-shifted objects are preserved for subsequent classification and rectification. As a complement to TGE and DCR, ExRPN provides better support for downstream classification and rectification.

Specifically, based on the K-FPN features used in NoOVD, we extract visual embeddings for proposals from the RPN and obtain proposal representations via RoI Align. We then design a two-stage textual prompting process for coarse domain estimation and foreground confidence reweighting.

Stage 1: domain estimation. We randomly sample a subset of proposal features and compute their similarities to the text embeddings of predefined domain descriptors introduced in TGE (e.g., a rainy image, a foggy image), pre-extracted by the frozen text encoder. Based on these similarities, we estimate the coarse domain attribute of the input image.

Stage 2: semantic prompting and foreground scoring. Conditioned on the estimated domain, we use the coarse-grained foreground and background prompts pre-generated by an LLM in NoOVD and compute their cosine similarities with all proposal embeddings. The similarity to the foreground prompt is treated as the foreground confidence, denoted as \hat{S}_{Foreg} .

We fuse the semantic foreground confidence with S_{RPN} to obtain the adaptive proposal confidence:

$$S_{\text{ExRPN}} = \alpha \cdot S_{\text{RPN}} + (1 - \alpha) \cdot \hat{S}_{\text{Foreg}}, \quad (8)$$

where $\alpha \in [0, 1]$ is a balancing coefficient.

Finally, we replace the original RPN confidence with S_{ExRPN} for proposal ranking and filtering. Specifically, proposals are sorted by the adapted confidence in descending order, and the top- K ones (set to 1,000, following Faster R-CNN) are retained and fed into the RoI head. In this way, ExRPN improves the probability that proposals containing novel and domain-shifted objects survive post-processing, thereby enhancing proposal recall under cross-category and cross-domain settings with negligible computational overhead, while providing more sufficient effective candidates for subsequent classification and rectification.

3.5 Implementation Details

We extract visual embeddings of base categories from the RoI classification head of a trained F-ViT detector and build category prototypes. Then, through TGE, we generate augmented visual embeddings covering novel categories and multiple visual domains, with **500 multi-domain embeddings for each category**. Notably, DCR training requires neither the participation of the detector nor any real data; we train this lightweight DCR module solely with the pre-extracted category prototypes and their extrapolated variants.

The overall objective of DCR consists of the visual rectification branch (DCR_V) and the semantic rectification branch (DCR_T):

$$\mathcal{L}_{\text{total}} = \mathcal{L}_{\text{DCR_V}} + \mathcal{L}_{\text{DCR_T}}. \quad (9)$$

For the DCR_V loss in Eq. (6), we set $\lambda_1 = 1$, $\lambda_2 = 1$, and $\lambda_3 = 1$. For the contrastive loss in Eq. (5), the temperature coefficient is set to $\tau = 0.7$. For ExRPN in Eq. (8), we follow NoOVD [51] and set the confidence fusion coefficient to $\alpha = 0.5$.

We train DCR on OV-LVIS for 30 epochs on a **single NVIDIA RTX 3090 GPU** with a batch size of 256. AdamW is used as the optimizer, with an initial learning rate of 10^{-4} and a weight decay of 0.1. The total training time is **only about 30 minutes**.

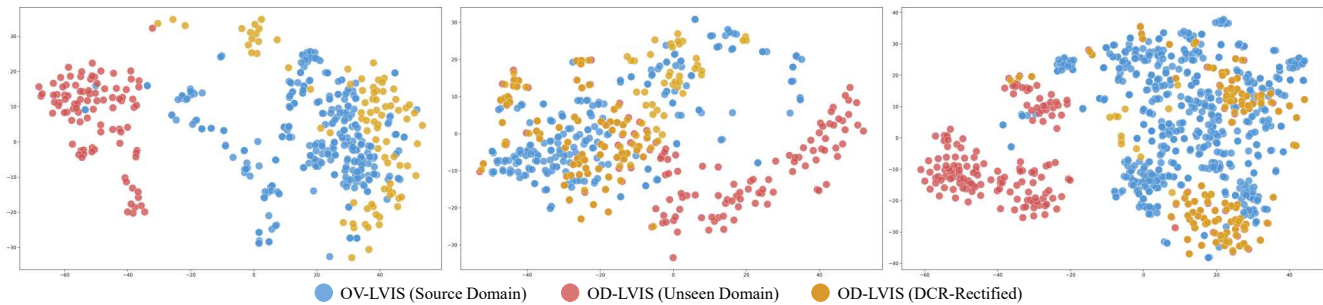


Figure 3: Visualization of OV-LVIS and OD-LVIS object embeddings. After applying DCR, the OD-LVIS embeddings (yellow) are pulled closer to the OV-LVIS source-domain embeddings (blue) than the original OD-LVIS embeddings (red).

4 Experiments

4.1 Setup

ODOV settings. Following ODOVD [52], models are trained on a single natural domain (*i.e.*, the OV-LVIS training set) and evaluated on all 15 open domains in OD-LVIS, consistent with the SDGOD setting. For open-vocabulary evaluation, we use the same category split: 405 *frequent* and 461 *common* categories as base categories for training, and 337 *rare* categories as novel categories for testing.

Evaluation methods. We select several mainstream VLM-based OVD methods and an ODOVD method for comparison on OD-LVIS. Specifically, we include the transfer learning approaches, *i.e.*, F-VLM [18], OWL-ViT [27], F-ViT (CLIPSelf [42] and DeCLIP [36] as the backbones), MM-OVOD [48], and OV-DQUO [35], and several knowledge distillation methods, *i.e.*, RKDWTF [1], DK-DETR [21], RegionCLIP [55], and region-aware training method YOLO-World [4], YOLOE [34]. We also incorporate the ODOV detection method DVtor [52]. We also include eight recent DG methods, ALT [8], ABA [3], NP [7], MAD [45], MixStyle [56], OA-DG [19], SRA [44] and PhysAug [47] for comparison.

Evaluation metrics. For evaluation, AP_f and AP_c denote average precision on *frequent* and *common* categories, respectively, while AP_r denotes average precision on *rare* categories. The overall average precision is denoted as AP .

4.2 Main Results on OD-LVIS

Comparison with ODOVD and OVD methods on OD-LVIS.

Table 1 compares our method with ODOVD and OVD methods on OD-LVIS. Our method achieves the best overall performance across multiple detector instantiations. Built upon F-ViT (DeCLIP ViT-L/14, 304.43M), ExDet attains the best results among all compared methods, reaching 25.3%, 24.7%, 26.3%, and 25.2% on the *frequent*, *common*, *rare*, and overall categories, respectively. Compared with the corresponding F-ViT (DeCLIP) baseline, this yields gains of 2.3%, 3.0%, 4.9%, and 3.0%; compared with DVtor, the gains remain 0.4%, 2.1%, 3.1%, and 1.6%, respectively. Our method also generalizes well to smaller backbones. With F-ViT (DeCLIP ViT-B/16, 86.26M), ExDet improves the baseline by 1.6%, 6.0%, 4.1%, and 3.9% on *frequent*, *common*, *rare*, and overall AP , respectively, and surpasses DVtor by 4.2%, 1.8%, and 2.1% on *common*, *rare*, and overall AP . When integrated into F-VLM (CLIP RN50×16, 167.33M), our method improves the baseline by 1.1%, 4.4%, 5.3%, and 3.2% on

Table 1: Comparison with SOTA on OD-LVIS (%).

Method	Backbone	Training Data	AP_f	AP_c	AP_r	AP
RegionCLIP [55]	RN50*	CC3M	16.6	13.0	9.7	13.9
	RN50×4*		19.5	15.8	12.4	16.7
OWL-ViT [27]	ViT-B/16	O365 + VG	13.1	13.9	13.2	13.5
	ViT-L/14		22.1	21.6	19.9	21.5
RKDWTF [1]	RN50* Base	LVIS-base + IN-L	14.6	12.4	8.7	12.6
	RN50* RKDPIS		13.4	12.1	10.3	12.3
	RN50* WTF		14.0	12.5	11.3	12.9
	RN50* WTF8x		15.8	14.3	11.9	14.5
DK-DETR [21]	RN50	LVIS-all	21.1	19.4	15.3	19.4
MM-OVOD [48]	RN50* (Agg)	LVIS-base	20.5	19.8	14.0	19.0
		LVIS-base + IN-L	20.4	20.4	15.9	19.6
YOLO-World [4]	YOLOv8-L*	O365 + GoldG	21.9	19.1	19.3	20.2
YOLOE [34]	YOLOv11-L*		13.7	8.6	6.8	10.3
OV-DQUO [35]	ViT-B/16		12.8	14.8	14.8	14.0
	ViT-L/14		16.4	20.6	21.2	19.1
F-VLM (CLIP) [18]	RN50×16		16.7	14.4	13.7	15.2
DVtor (CLIP) [52]			17.6	16.9	15.8	17.0
ExDet (CLIP)			17.8	18.8	19.0	18.4
F-ViT (CLIPSelf) [42]			17.1	12.0	12.2	14.0
DVtor (CLIPSelf) [52]	ViT-B/16	LVIS-base	19.0	14.3	14.0	16.1
ExDet (CLIPSelf)			19.2	18.0	16.1	18.1
F-ViT (CLIPSelf) [42]	ViT-L/14		22.5	21.3	20.2	21.6
DVtor (CLIPSelf) [52]			23.9	22.9	21.6	23.1
ExDet (CLIPSelf)	23.9	24.3	25.9	24.5		
F-ViT (DeCLIP) [36]	ViT-B/16		17.8	12.9	13.2	14.9
DVtor (DeCLIP) [52]			19.5	14.7	15.5	16.7
ExDet (DeCLIP)			19.4	18.9	17.3	18.8
F-ViT (DeCLIP) [36]			23.0	21.7	21.4	22.2
DVtor (DeCLIP) [52]	ViT-L/14	24.9	22.7	23.2	23.6	
ExDet (DeCLIP)		25.3	24.7	26.3	25.2	

Notes: IN-L denotes the inclusion of images corresponding to the 997 categories shared between ImageNet-21k-P [30] and LVIS [10], "*" indicates that the backbone is not initialized with CLIP, O365 is an abbreviation for Objects365 [31], CC3M [32], GoldG [15], and VG [17] are all publicly available datasets.

Table 2: Comparison of DG methods on OD-LVIS (%).

Method	AP_f	AP_c	AP_r	AP
F-ViT (DeCLIP) (ViT-B/16)	17.8	12.9	13.2	14.9
+ ALT [8]	18.2	13.2	13.1	15.1
+ ABA [3]	18.0	13.4	13.8	15.3
+ NP [7]	18.6	14.0	14.2	15.8
+ MAD [45]	18.8	13.9	14.1	15.9
+ MixStyle [56]	17.9	13.3	13.5	15.1
+ OA-DG [19]	17.2	14.5	13.2	15.3
+ SRA [44]	16.9	14.2	14.0	15.2
+ PhysAug [47]	18.3	13.6	13.7	15.5
DVtor [52]	19.5	14.7	15.5	16.7
ExDet	19.4	18.9	17.3	18.8

frequent, *common*, *rare*, and overall AP , respectively, and outperforms DVtor by 1.9%, 3.2%, and 1.4% on *common*, *rare*, and overall AP . Across different detector variants, ExDet consistently outperforms the corresponding baselines and DVtor, verifying the strong transferability of DCR and ExRPN, as well as their effectiveness in improving open-domain open-vocabulary generalization.

Table 3: Comparative results on OV-LVIS (%).

Method	Backbone	Training Data	AP_f	AP_c	AP_r	AP
RegionCLIP [55]	RN50*	CC3M	34.0	27.4	17.1	28.2
	RN50×4*		36.9	32.1	22.0	32.3
OWL-ViT [27]	ViT-B/16 ViT-L/14	O365 + VG	-	-	20.6 31.2	27.2 34.6
RKD WTF [1]	RN50* Base RN50* RKDPIS RN50* WTF RN50* WTF8x	LVIS-base + IN-L	26.4	19.4	12.2	20.9
			25.5	20.9	17.3	22.1
			26.7	21.4	17.1	22.8
			29.1	25.0	21.1	25.9
MM-OVOD [48]	RN50* (Agg)	LVIS-base	-	-	19.3	30.6
		LVIS-base + IN-L	-	-	27.3	33.1
DK-DETR [21]	RN50	LVIS-all	40.2	32.0	22.2	33.5
YOLO-World [4]	YOLOv8-L*	O365 + GoldG	35.4	24.9	22.9	28.7
YOLOE [34]	YOLOv11-L*		36.5	35.0	29.1	35.2
OV-DQUO [35]	ViT-B/16 ViT-L/14		23.8 28.5	27.7 36.0	29.4 39.5	26.5 33.7
F-VLM (CLIP) [18] DVtor (CLIP) [52] ExDet (CLIP)	RN50×16		- - 33.0	- - 34.1	30.4 33.1	32.1 33.5
F-ViT (CLIPSelf) [42] DVtor (CLIPSelf) [52] ExDet (CLIPSelf)	ViT-B/16	LVIS-base	29.1 30.4	21.8 23.2	25.3 26.3	25.2 26.6
F-ViT (CLIPSelf) [42] DVtor (CLIPSelf) [52] ExDet (CLIPSelf)	ViT-L/14		35.6 36.9	34.6 35.8	34.9 36.4	35.1 36.3
F-ViT (DeCLIP) [36] DVtor (DeCLIP) [52] ExDet (DeCLIP)	ViT-B/16		29.8 31.0	22.4 23.7	26.8 28.1	26.0 27.3
F-ViT (DeCLIP) [36] DVtor (DeCLIP) [52] ExDet (DeCLIP)	ViT-L/14		36.5 37.6	35.2 35.9	37.2 39.0	36.0 37.1
			38.2	37.0	40.1	38.0

Table 4: Cross-dataset results on Objects365 (%).

Method	Backbone	Training Data	AP_r	AP
Detic [57]	RN50*	LVIS-all	9.5	13.9
		LVIS-all + IN-L	12.4	15.6
MM-OVOD [48]		LVIS-all	10.1	14.8
		LVIS-all + IN-L	13.1	16.6
F-VLM (CLIP) [18] DVtor (CLIP) [52] ExDet (CLIP)	RN50×16		14.9 16.2	16.2 17.9
F-ViT (CLIPSelf) [42] DVtor (CLIPSelf) [52] ExDet (CLIPSelf)	ViT-B/16		16.8 17.5	19.0 19.8
F-ViT (CLIPSelf) [42] DVtor (CLIPSelf) [52] ExDet (CLIPSelf)	ViT-L/14	LVIS-base	21.7 22.3	23.7 24.0
F-ViT (DeCLIP) [36] DVtor (DeCLIP) [52] ExDet (DeCLIP)	ViT-B/16		17.6 18.7	20.2 21.1
F-ViT (DeCLIP) [36] DVtor (DeCLIP) [52] ExDet (DeCLIP)	ViT-L/14		22.3 23.7	24.5 25.0
			25.1	26.2

Table 5: Cross-dataset results on MSOSB (%).

Method	Backbone	Training Data	AP_r	AP
F-VLM (CLIP) [18] DVtor (CLIP) [52] ExDet (CLIP)	RN50×16		31.3 32.8	37.2 39.0
F-ViT (CLIPSelf) [42] DVtor (CLIPSelf) [52] ExDet (CLIPSelf)	ViT-B/16		29.8 31.4	35.6 37.2
F-ViT (CLIPSelf) [42] DVtor (CLIPSelf) [52] ExDet (CLIPSelf)	ViT-L/14	LVIS-base	38.2 39.8	42.6 43.9
F-ViT (DeCLIP) [36] DVtor (DeCLIP) [52] ExDet (DeCLIP)	ViT-B/16		30.8 32.5	36.3 37.9
F-ViT (DeCLIP) [36] DVtor (DeCLIP) [52] ExDet (DeCLIP)	ViT-L/14		38.8 40.1	43.3 45.0
			41.5	45.7

As shown in Fig. 3, we visualize object embeddings of three representative categories from OV-LVIS, OD-LVIS, and DCR-rectified OD-LVIS. Compared with the original OD-LVIS embeddings, the

DCR-rectified embeddings are clearly closer to the OV-LVIS source-domain clusters. This shows that DCR effectively narrows the visual embedding distribution gap and improves feature compatibility for cross-domain classification.

Comparison with DG methods on OD-LVIS Table 2 compares our method with F-ViT and eight DG methods on OD-LVIS under the same DeCLIP ViT-B/16 backbone. ExDet achieves the best overall performance, obtaining 19.4%, 18.9%, 17.3%, and 18.8% on the *frequent*, *common*, *rare*, and overall categories, respectively. Compared with F-ViT and DVtor, it improves the overall AP by 3.9 and 2.1 points, respectively, with especially notable gains on the *common* and *rare* categories. This verifies the strong transferability and generalization ability of our method under domain shifts.

4.3 Additional Evaluation on OV-LVIS

Table 3 reports the comparison on the OV-LVIS validation set. ExDet consistently achieves the best overall performance across multiple detector instantiations. In particular, built upon F-ViT (DeCLIP ViT-L/14), it delivers the best results among all compared methods, reaching 38.2%, 37.0%, 40.1%, and 38.0% on *frequent*, *common*, *rare*, and overall categories, respectively. Relative to the corresponding F-ViT (DeCLIP) baseline, this yields gains of 1.7%, 1.8%, 2.9%, and 1.4%; relative to DVtor, the gains remain 0.6%, 1.1%, 1.1%, and 0.9%, respectively. ExDet also generalizes well to smaller backbones. With F-ViT (DeCLIP ViT-B/16), it improves the baseline by 1.8%, 2.9%, 3.7%, and 3.4% on AP_f , AP_c , AP_r , and overall AP , respectively, and surpasses DVtor by 0.6%, 3.4%, 2.4%, and 2.1%. With F-ViT (CLIPSelf ViT-L/14), ExDet achieves 38.1%, 37.0%, 39.7%, and 37.9%, improving the baseline by 2.5%, 2.4%, 4.8%, and 2.8%, and DVtor by 1.2%, 1.2%, 3.3%, and 1.6%, respectively. Even under the RN50×16 setting, it improves F-VLM by 0.5%, 2.5%, 4.6%, and 1.5% on AP_f , AP_c , AP_r , and overall AP , respectively, while still outperforming DVtor by 0.5%, 1.5%, 1.9%, and 1.2%. Although the domain gap in OV-LVIS is less pronounced than that in OD-LVIS, ExDet still brings consistent gains across different detectors and backbones. This indicates that the proposed framework not only improves robustness to domain variations, but also enhances novel-category generalization by leveraging category- and domain-aware proxy visual prototypes together with Detector-Compatible Rectification.

4.4 Cross-dataset Generalization Results

Main results on Objects365. Table 4 reports the cross-dataset transfer results from OV-LVIS to Objects365, where all models are directly evaluated on the validation set without adaptation. Following MM-OVOD, we define the bottom one-third categories by frequency as *rare* categories. Detic and MM-OVOD are trained on LVIS-all, with the In-L variants further using ImageNet-21k-P [30], while F-ViT, DVtor, and ExDet are trained only on the OV-LVIS base categories. ExDet achieves the best transfer performance across different backbones and VLM initializations. With F-ViT (DeCLIP ViT-L/14), it reaches 25.1% AP_r and 26.2% AP , surpassing the baseline by 2.8% and 1.7%, and DVtor by 1.4% and 1.2%, respectively. Similar gains are observed under CLIP and CLIPSelf settings. Although smaller than on OD-LVIS and OV-LVIS, these improvements remain consistent, confirming better cross-dataset robustness and novel-category generalization.

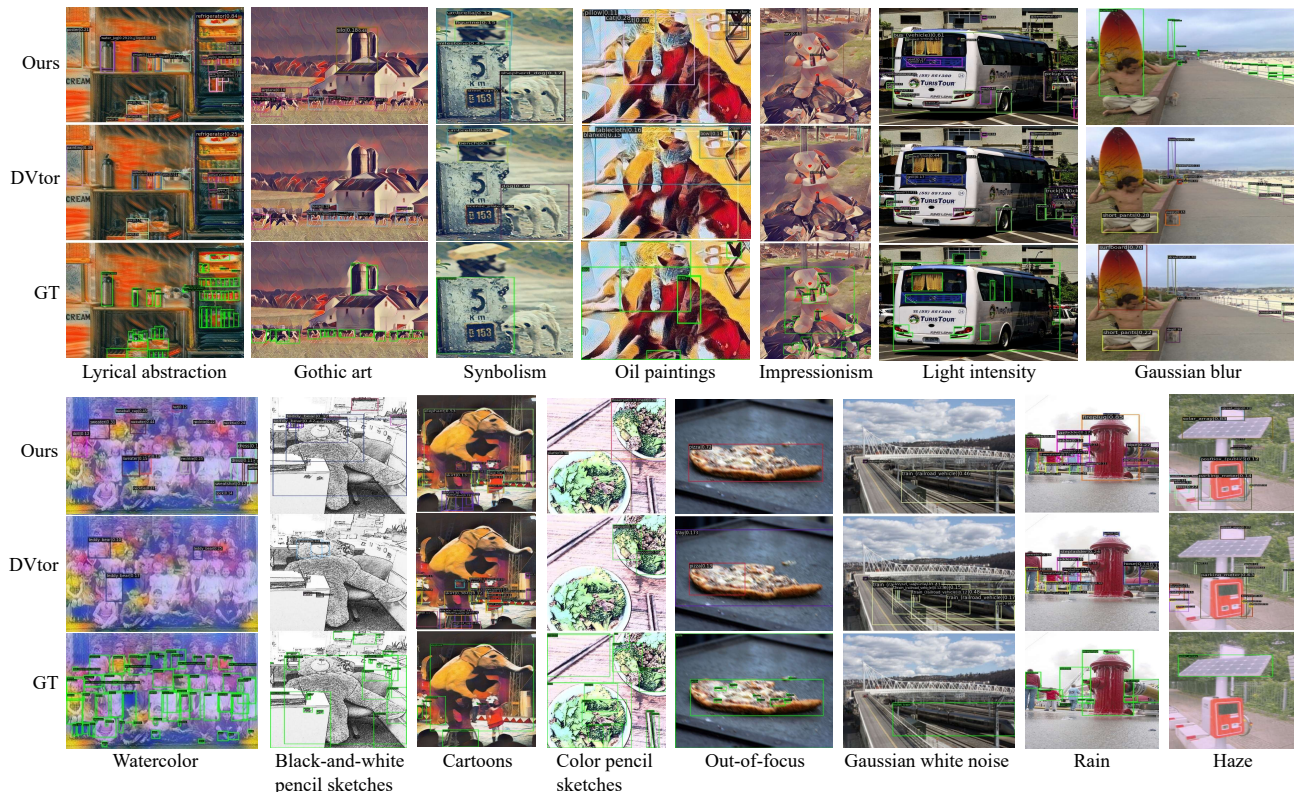


Figure 4: Qualitative comparison of our method, DVtor, and GT under diverse domain shifts and challenging imaging conditions.

Table 6: Ablation study results on OD-LVIS (%).

Method	AP_f	AP_c	AP_r	AP
F-ViT (DeCLIP) (ViT-B/16)	17.8	12.9	13.2	14.9
+ DCR_V	18.2	15.8	14.2	16.5
+ DCR_T	18.6	14.7	16.2	16.5
+ DCR_V + DCR_T	18.8	16.9	16.7	17.6
+ ExRPN	18.2	14.3	15.6	16.0
ExDet (DCR_V + DCR_T + ExRPN)	19.4	18.9	17.3	18.8

Main results on MSOSB. MSOSB is a multi-style benchmark with 5 visual styles and the same 80 categories as COCO. Following category frequency, we treat the 20 less frequent categories as *rare* and the remaining 60 as regular. Table 5 reports the corresponding cross-dataset transfer results, where all models are directly tested without finetuning. ExDet achieves the best performance across all settings. With F-ViT (DeCLIP ViT-L/14), it reaches 41.5% AP_r and 45.7% AP , surpassing the baseline by 2.7% and 2.4%, and DVtor by 1.4% and 0.7%, respectively. Similar gains are observed with CLIP and CLIPSelf, confirming strong generalization to unseen datasets and visual styles without target-dataset adaptation.

4.5 Ablation Study

Component analysis. Table 6 reports the ablation results for F-ViT (DeCLIP ViT-B/16) on OD-LVIS to evaluate the contributions of DCR_V, DCR_T, and ExRPN. Each component improves the baseline. DCR_V raises AP from 14.9% to 16.5%, while DCR_T achieves the same gain and improves rare categories (16.2% vs. 14.2%). Combining DCR_V and DCR_T further improves AP to 17.6%, showing their complementarity for cross-domain novel-category detection. ExRPN alone improves the baseline to 16.0% AP , with clear gains

on both common and rare categories, showing its effectiveness in improving proposal quality under domain shift. The full model performs best, reaching 19.4%, 18.9%, 17.3%, and 18.8% on AP_f , AP_c , AP_r , and AP , respectively. This confirms that DCR and ExRPN are complementary: the former improves category- and domain-aware representation alignment, while the latter strengthens localization and recall in unseen domains.

Inference efficiency analysis. We evaluate speed on a single RTX 3090 GPU. The baseline F-ViT (DeCLIP ViT-B/16) runs at 21.18 FPS, while the full model with DCR and ExRPN achieves 12.55 FPS. Despite the extra overhead, it improves overall AP by 3.9%, showing a reasonable accuracy–efficiency trade-off. Under the same setting, MM-OVOD and OV-DQUO run at 2.09 FPS and 2.31 FPS, respectively, while DVtor achieves 15.17 FPS. Although our method is moderately slower than DVtor, it delivers higher accuracy and remains substantially more efficient than other methods.

Advantages of ExRPN. To evaluate ExRPN’s **Table 7: Recall coverage of open-domain open-vocabulary objects, we use $Recall@IoU \geq 0.5$.** As shown in Table 7, on OD-LVIS with F-ViT (DeCLIP ViT-B/16), Ex-RPN consistently outperforms both R-RPN and the original RPN in rare-category recall AR_r and overall recall AR .

Method	AR_r	AR
RPN	53.9	56.2
R-RPN	58.6	61.1
ExRPN	63.2	65.5

5 Visualized Results

In Fig. 4, we visualize the detection results of GT, DVtor, and our method under diverse domain shifts and imaging degradations. Compared with DVtor, our method detects more objects with more

accurate localization, showing stronger robustness and generalization in ODOVD. Under style shifts such as lyrical abstraction, gothic art, symbolism, oil paintings, watercolor, and cartoons, DVtor often misses meaningful objects or produces incomplete detections, whereas our method identifies more relevant objects. Similar gains are observed under challenging conditions, including Gaussian blur, Gaussian white noise, rain, haze, and out-of-focus degradation, where our method preserves better recall and localization quality. These results suggest that ExDet is more robust to both domain variation and image corruption. Nevertheless, compared with GT, it still misses some objects in highly challenging scenarios, indicating that ODOVD remains difficult and that object coverage and recognition accuracy still have room for improvement.

6 Conclusion

We propose ExDet, a lightweight framework for ODOVD. Built upon a frozen CLIP-based two-stage detector, ExDet consists of Text-Guided Extrapolation (TGE), Detector-Compatible Rectification (DCR), and ExRPN. TGE infers category- and domain-aware proxy visual prototypes from text. DCR is learned independently under the supervision of these enhanced prototypes in a detector training-free and real-data-free manner, and rectifies post-classification-head representations toward a detector-compatible source-domain visual distribution during inference, thereby improving recognition of novel categories and unseen domains. As a complementary inference-time strategy, ExRPN recalibrates proposal confidence to improve recall for novel and domain-shifted objects. Experiments on OD-LVIS, OV-LVIS, Objects365, and MSOSB demonstrate that our method achieves SOTA performance and strong category-domain generalization.

References

- [1] Hanoona Bangalath, Muhammad Maaz, Muhammad Uzair Khattak, Salman H Khan, and Fahad Shahbaz Khan. 2022. Bridging the gap between object and image-level representations for open-vocabulary detection. *Advances in Neural Information Processing Systems* 35 (2022), 33781–33794.
- [2] Haibo Chen, Zhoujie Wang, Lei Zhao, Jun Li, and Jian Yang. 2025. Trst: Arbitrary high-quality text-guided style transfer with transformers. *IEEE Transactions on Image Processing* (2025).
- [3] Sheng Cheng, Tejas Gokhale, and Yezhou Yang. 2023. Adversarial Bayesian Augmentation for Single-Source Domain Generalization. In *Proceedings of the IEEE/CVF International Conference on Computer Vision*. 11400–11410.
- [4] Tianheng Cheng, Lin Song, Yixiao Ge, Wenyu Liu, Xinggang Wang, and Ying Shan. 2024. Yolo-world: Real-time open-vocabulary object detection. In *Proceedings of the IEEE/CVF Conference on Computer Vision and Pattern Recognition*. 16901–16911.
- [5] Muhammad Sohail Danish, Muhammad Haris Khan, Muhammad Akhtar Munir, M Saquib Sarfraz, and Mohsen Ali. 2024. Improving single domain-generalized object detection: A focus on diversification and alignment. In *Proceedings of the IEEE/CVF Conference on Computer Vision and Pattern Recognition*. 17732–17742.
- [6] Yu Du, Fangyun Wei, Ziheng Zhang, Miaojing Shi, Yue Gao, and Guoqi Li. 2022. Learning to prompt for open-vocabulary object detection with vision-language model. In *Proceedings of the IEEE/CVF Conference on Computer Vision and Pattern Recognition*. 14084–14093.
- [7] Qi Fan, Mattia Segu, Yu-Wing Tai, Fisher Yu, Chi-Keung Tang, Bernt Schiele, and Dengxin Dai. 2023. Towards robust object detection invariant to real-world domain shifts. In *The Eleventh International Conference on Learning Representations (ICLR 2023)*.
- [8] Tejas Gokhale, Rushil Anirudh, Jayaraman J Thiagarajan, Bhavya Kailkhura, Chitta Baral, and Yezhou Yang. 2023. Improving diversity with adversarially learned transformations for domain generalization. In *Proceedings of the IEEE/CVF Winter Conference on Applications of Computer Vision*. 434–443.
- [9] Xiuye Gu, Tsung-Yi Lin, Weicheng Kuo, and Yin Cui. 2021. Open-vocabulary object detection via vision and language knowledge distillation. *arXiv preprint arXiv:2104.13921* (2021).
- [10] Agrim Gupta, Piotr Dollar, and Ross Girshick. 2019. Lvis: A dataset for large vocabulary instance segmentation. In *Proceedings of the IEEE/CVF conference on computer vision and pattern recognition*. 5356–5364.
- [11] Jianhong Han, Yupei Wang, and Liang Chen. 2025. Style-Adaptive Detection Transformer for Single-Source Domain Generalized Object Detection. *arXiv preprint arXiv:2504.20498* (2025).
- [12] Seongmin Hwang, Daeyoung Han, and Moongu Jeon. 2025. DG-DETR: Toward Domain Generalized Detection Transformer. *arXiv preprint arXiv:2504.19574* (2025).
- [13] Joonhyun Jeong, Geondo Park, Jayeon Yoo, Hyungsik Jung, and Heesu Kim. 2024. ProxyDet: Synthesizing Proxy Novel Classes via Classwise Mixup for Open-Vocabulary Object Detection. In *Proceedings of the AAAI Conference on Artificial Intelligence*, Vol. 38. 2462–2470.
- [14] Chao Jia, Yinfei Yang, Ye Xia, Yi-Ting Chen, Zarana Parekh, Hieu Pham, Quoc Le, Yun-Hsuan Sung, Zhen Li, and Tom Duerig. 2021. Scaling up visual and vision-language representation learning with noisy text supervision. In *International conference on machine learning*. 4904–4916.
- [15] Aishwarya Kamath, Mannat Singh, Yann LeCun, Gabriel Synnaeve, Ishan Misra, and Nicolas Carion. 2021. Mdetr-modulated detection for end-to-end multimodal understanding. In *Proceedings of the IEEE/CVF international conference on computer vision*. 1780–1790.
- [16] Dahun Kim, Anelia Angelova, and Weicheng Kuo. 2023. Region-aware pretraining for open-vocabulary object detection with vision transformers. In *Proceedings of the IEEE/CVF conference on computer vision and pattern recognition*. 11144–11154.
- [17] Ranjay Krishna, Yuke Zhu, Oliver Groth, Justin Johnson, Kenji Hata, Joshua Kravitz, Stephanie Chen, Yannis Kalantidis, Li-Jia Li, David A Shamma, et al. 2017. Visual genome: Connecting language and vision using crowdsourced dense image annotations. *International journal of computer vision* 123 (2017), 32–73.
- [18] Weicheng Kuo, Yin Cui, Xiuye Gu, AJ Piergiovanni, and Anelia Angelova. 2022. Fvlm: Open-vocabulary object detection upon frozen vision and language models. *arXiv preprint arXiv:2209.15639* (2022).
- [19] Wooju Lee, Dasol Hong, Hyungtae Lim, and Hyun Myung. 2024. Object-aware domain generalization for object detection. In *proceedings of the AAAI conference on artificial intelligence*, Vol. 38. 2947–2955.
- [20] Jiaming Li, Jiacheng Zhang, Jichang Li, Ge Li, Si Liu, Liang Lin, and Guanbin Li. 2024. Learning background prompts to discover implicit knowledge for open vocabulary object detection. In *Proceedings of the IEEE/CVF Conference on Computer Vision and Pattern Recognition*. 16678–16687.
- [21] Liangqi Li, Jiaxu Miao, Dahu Shi, Wenming Tan, Ye Ren, Yi Yang, and Shiliang Pu. 2023. Distilling detr with visual-linguistic knowledge for open-vocabulary object detection. In *Proceedings of the IEEE/CVF International Conference on Computer Vision*. 6501–6510.
- [22] Chuang Lin, Zehuan Yuan, Sicheng Zhao, Peize Sun, Changhu Wang, and Jianfei Cai. 2021. Domain-invariant disentangled network for generalizable object detection. In *Proceedings of the IEEE/CVF international conference on computer vision*. 8771–8780.
- [23] Xudong Liu, Zikun Chen, Ruowei Jiang, Ziyi Wu, Kejia Yin, Han Zhao, Parham Aarabi, and Igor Gilitschenski. 2025. S²Edit: Text-Guided Image Editing with Precise Semantic and Spatial Control. *arXiv preprint arXiv:2507.04584* (2025).
- [24] Yajing Liu, Shijun Zhou, Xiyao Liu, Chunhui Hao, Baojie Fan, and Jiandong Tian. 2024. Unbiased faster r-cnn for single-source domain generalized object detection. In *Proceedings of the IEEE/CVF conference on computer vision and pattern recognition*. 28838–28847.
- [25] Yueming Lyu, Tianwei Lin, Fu Li, Dongliang He, Jing Dong, and Tieniu Tan. 2023. Deltaedit: Exploring text-free training for text-driven image manipulation. *arXiv preprint arXiv:2303.06285* (2023).
- [26] Yueming Lyu, Kang Zhao, Bo Peng, Yue Jiang, Yingya Zhang, and Jing Dong. 2023. DeltaSpace: A Semantic-aligned Feature Space for Flexible Text-guided Image Editing. *arXiv preprint arXiv:2310.08785* (2023).
- [27] M Minderer, A Gritsenko, A Stone, M Neumann, D Weissenborn, A Dosovitskiy, A Mahendran, A Arnab, M Dehghani, Z Shen, et al. 2022. Simple open-vocabulary object detection with vision transformers. *arXiv 2022. arXiv preprint arXiv:2205.06230* 2 (2022).
- [28] Alec Radford, Jong Wook Kim, Chris Hallacy, Aditya Ramesh, Gabriel Goh, Sandhini Agarwal, Girish Sastry, Amanda Askell, Pamela Mishkin, Jack Clark, et al. 2021. Learning transferable visual models from natural language supervision. In *International conference on machine learning*. 8748–8763.
- [29] Zhijie Rao, Jingcai Guo, Luyao Tang, Yue Huang, Xinghao Ding, and Song Guo. 2024. Srdc: Semantic reasoning with compound domains for single-domain generalized object detection. *IEEE Transactions on Neural Networks and Learning Systems* (2024).
- [30] Tal Ridnik, Emanuel Ben-Baruch, Asaf Noy, and Lihi Zelnik-Manor. 2021. Imagenet-21k pretraining for the masses. *arXiv preprint arXiv:2104.10972* (2021).
- [31] Shuai Shao, Zeming Li, Tianyuan Zhang, Chao Peng, Gang Yu, Xiangyu Zhang, Jing Li, and Jian Sun. 2019. Objects365: A large-scale, high-quality dataset for object detection. In *Proceedings of the IEEE/CVF international conference on computer vision*. 8430–8439.
- [32] Piyush Sharma, Nan Ding, Sebastian Goodman, and Radu Soricut. 2018. Conceptual captions: A cleaned, hypernymed, image alt-text dataset for automatic image captioning. In *Proceedings of the 56th Annual Meeting of the Association for Computational Linguistics (Volume 1: Long Papers)*. 2556–2565.
- [33] Vidit Vidit, Martin Engilberge, and Mathieu Salzmann. 2023. Clip the gap: A single domain generalization approach for object detection. In *Proceedings of the IEEE/CVF conference on computer vision and pattern recognition*. 3219–3229.
- [34] Ao Wang, Lihao Liu, Hui Chen, Zijia Lin, Jungong Han, and Guiguang Ding. 2025. Yoloec: Real-time seeing anything. *arXiv preprint arXiv:2503.07465* (2025).
- [35] Junjie Wang, Bin Chen, Bin Kang, Yulin Li, Weizhi Xian, Yichi Chen, and Yong Xu. 2025. Ov-dqo: Open-vocabulary detr with denoising text query training and open-world unknown objects supervision. In *Proceedings of the AAAI Conference on Artificial Intelligence*, Vol. 39. 7762–7770.
- [36] Junjie Wang, Bin Chen, Yulin Li, Bin Kang, Yichi Chen, and Zhuotao Tian. 2025. DeCLIP: Decoupled Learning for Open-Vocabulary Dense Perception. In *Proceedings of the Computer Vision and Pattern Recognition Conference*. 14824–14834.
- [37] Jiacheng Wang, Ping Liu, Jingen Liu, and Wei Xu. 2023. Text-guided eyeglasses manipulation with spatial constraints. *IEEE Transactions on Multimedia* 26 (2023), 4375–4388.
- [38] Luting Wang, Yi Liu, Penghui Du, Zihan Ding, Yue Liao, Qiaosong Qi, Biaolong Chen, and Si Liu. 2023. Object-aware distillation pyramid for open-vocabulary object detection. In *Proceedings of the IEEE/CVF Conference on Computer Vision and Pattern Recognition*. 11186–11196.
- [39] Aming Wu and Cheng Deng. 2022. Single-domain generalized object detection in urban scene via cyclic-disentangled self-distillation. In *Proceedings of the IEEE/CVF Conference on computer vision and pattern recognition*. 847–856.
- [40] Fan Wu, Jinling Gao, Lanqing Hong, Xinbing Wang, Chenghu Zhou, and Nanyang Ye. 2024. G-NAS: Generalizable Neural Architecture Search for Single Domain Generalization Object Detection. In *Proceedings of the AAAI Conference on Artificial Intelligence*, Vol. 38. 5958–5966.
- [41] Fei Wu, Yongheng Ma, Hao Jin, Xiao-Yuan Jing, and Guo-Ping Jiang. 2023. MFE-CLIP: CLIP with mapping-fusion embedding for text-guided image editing. *IEEE Signal Processing Letters* 31 (2023), 116–120.
- [42] Size Wu, Wenwei Zhang, Lumin Xu, Sheng Jin, Xiangtai Li, Wentao Liu, and Chen Change Loy. 2023. Clipself: Vision transformer distills itself for open-vocabulary dense prediction. *arXiv preprint arXiv:2310.01403* (2023).
- [43] Xiaoshi Wu, Feng Zhu, Rui Zhao, and Hongsheng Li. 2023. Cora: Adapting clip for open-vocabulary detection with region prompting and anchor pre-matching. In *Proceedings of the IEEE/CVF conference on computer vision and pattern recognition*. 7031–7040.
- [44] Anqi Xiao, Weichen Yu, and Hongyuan Yu. 2025. Sample-Aware RandAugment: Search-Free Automatic Data Augmentation for Effective Image Recognition: A.

- Xiao et al. *International Journal of Computer Vision* 133, 11 (2025), 7710–7725.
- [45] Mingjun Xu, Lingyun Qin, Weijie Chen, Shiliang Pu, and Lei Zhang. 2023. Multi-view adversarial discriminator: Mine the non-causal factors for object detection in unseen domains. In *Proceedings of the IEEE/CVF conference on computer vision and pattern recognition*. 8103–8112.
- [46] Shilin Xu, Xiangtai Li, Size Wu, Wenwei Zhang, Yunhai Tong, and Chen Change Loy. 2024. DST-Det: Open-Vocabulary Object Detection via Dynamic Self-Training. *IEEE Transactions on Circuits and Systems for Video Technology* (2024).
- [47] Xiaoran Xu, Jiangang Yang, Wenhui Shi, Siyuan Ding, Luqing Luo, and Jian Liu. 2025. PhysAug: A Physical-guided and Frequency-based Data Augmentation for Single-Domain Generalized Object Detection. In *Proceedings of the AAAI Conference on Artificial Intelligence*. 21815–21823.
- [48] Yifan Xu, Mengdan Zhang, Xiaoshan Yang, and Changsheng Xu. 2023. Exploring multi-modal contextual knowledge for open-vocabulary object detection. *arXiv preprint arXiv:2308.15846* (2023).
- [49] Alireza Zareian, Kevin Dela Rosa, Derek Hao Hu, and Shih-Fu Chang. 2021. Open-vocabulary object detection using captions. In *Proceedings of the IEEE/CVF Conference on Computer Vision and Pattern Recognition*. 14393–14402.
- [50] Haozhuo Zhang, Huimin Yu, Yuming Yan, and Runfa Wang. 2022. Gated domain-invariant feature disentanglement for domain generalizable object detection. *arXiv preprint arXiv:2203.11432* (2022).
- [51] Yupeng Zhang, Ruize Han, Zhiwei Chen, Wei Feng, and Liang Wan. 2026. NoOVD: Novel Category Discovery and Embedding for Open-Vocabulary Object Detection. [arXiv:2603.21069](https://arxiv.org/abs/2603.21069) [cs.CV] <https://arxiv.org/abs/2603.21069>
- [52] Yupeng Zhang, Ruize Han, Fangnan Zhou, Song Wang, Wei Feng, and Liang Wan. 2025. ODOV: Towards Open-Domain Open-Vocabulary Object Detection. Preprint submitted to arXiv on August 2, 2025; expected to be available shortly..
- [53] Yupeng Zhang, Shuqi Zheng, Ruize Han, Yuzhong Feng, Junhui Hou, Linqi Song, Wei Feng, and Liang Wan. [n. d.]. Rethinking the One-shot Object Detection: Cross-Domain Object Search. In *ACM Multimedia 2024*.
- [54] Shiyu Zhao, Samuel Schuster, Long Zhao, Zhixing Zhang, Yumin Suh, Manmohan Chandraker, Dimitris N Metaxas, et al. 2024. Taming self-training for open-vocabulary object detection. In *Proceedings of the IEEE/CVF Conference on Computer Vision and Pattern Recognition*. 13938–13947.
- [55] Yiwu Zhong, Jianwei Yang, Pengchuan Zhang, Chunyuan Li, Noel Codella, Lianian Harold Li, Luowei Zhou, Xiyang Dai, Lu Yuan, Yin Li, et al. 2022. Regionclip: Region-based language-image pretraining. In *Proceedings of the IEEE/CVF conference on computer vision and pattern recognition*. 16793–16803.
- [56] Kaiyang Zhou, Yongxin Yang, Yu Qiao, and Tao Xiang. 2024. Mixstyle neural networks for domain generalization and adaptation. *International Journal of Computer Vision* 132, 3 (2024), 822–836.
- [57] Xingyi Zhou, Rohit Girdhar, Armand Joulin, Philipp Krähenbühl, and Ishan Misra. 2022. Detecting twenty-thousand classes using image-level supervision. In *European Conference on Computer Vision*. 350–368.